Nonuniform dynamic gratings in photorefractive media with nonlocal response

S. Bugaychuk,[1] L. Kovács,[2] G. Mandula,[2] K. Polgár,[2] and R. A. Rupp[3]
[1]*Institute of Physics, National Academy of Science of Ukraine, e Prospect Nauki 46, 03039 Kiev, Ukraine*
[2]*Research Institute for Solid State Physics and Optics, Konkoly-Thege M. út 29-33, H-1121 Budapest, Hungary*
[3]*Institute for Experimental Physics, University of Vienna, Strudholgasse 4, A-1090 Vienna, Austria*
(Received 11 October 2002; revised manuscript received 23 December 2002; published 8 April 2003)

The amplitude of the phase dynamic grating is a nonuniform space distributed in photorefractive crystals with nonlocal response as a result of energy transfer between the interacted waves. The dynamical process of grating formation in the case of transmission two- and four-wave mixing is described by the damped sine-Gordon equation that governs the soliton propagation. A stationary soliton solution for the grating amplitude profile was obtained. Experiments on observation of a nonuniform distribution of the grating amplitude through the crystal volume are presented. It is experimentally shown that the changes of the grating amplitude profile in dependence of input intensity ratio match the solutions of the damped sine-Gordon equation in steady state. The diffraction efficiency of energy transfer is determined by the value of the integral under the grating amplitude profile. The soliton profile is altered with changing input intensity ratio of recorded beams. It provides the effect of diffraction efficiency management by changing the half-width and the position of the soliton. The theory predicts a multisoliton behavior in reversible media with strong amplitifcaiton gain that leads to auto-oscillations of output wave intensities.

DOI: 10.1103/PhysRevE.67.046603 PACS number(s): 42.65.Hw, 42.65.Sf, 42.40.Pa, 42.65.Tg

I. INTRODUCTION

The theory of the optical dynamic holography considers the effect resulting from the interaction of laser beams in nonlinear media, mostly in ferroelectric crystals. In a medium with nonlocal response the wave self-diffraction exhibits the effect of wave amplification being conditional on a phase shift between the interference pattern and the recorded grating [1,2]. Many applications in photonics are based on this effect [3–6]. Their conventional theoretical modeling is reduced to a set of nonlinear equations for the output wave intensities.

The processes of the dynamic wave mixing are based on the nonlinear properties of ferroelectric crystals and on the photorefractive effects [1–8]. An interference pattern of the interacting laser beams induces an internal space charge that is nonuniformly distributed in the crystals. The space-charge field modulates the refractive index. The same interacting waves create the refractive index grating and diffract from such grating during the self-diffraction process. The diffusion dominant photorefractive mechanism is a conventional one to record nonlocal gratings, which are shifted on the quarter of the space period relative to the light interference pattern. Because of the presence of the additional phase shift the well-known effect of the energy transfer between the coupled waves and amplification of one of them appear. Furthermore, the energy transfer leads to changes in the contrast of the interference pattern over the direction of wave propagation, because the wave intensities are changed inside the crystal. In this way the grating amplitude must change as well. The essentials of the nonuniform distribution of the grating amplitude across the crystal have already been described in the first papers devoted to the optical dynamic holography [8,9].

In the present paper we study the transmission four-wave mixing (FWM) in ferroelectric crystals. Our main interest lies in the investigation of the photoinduced grating inside the crystal. We have obtained that the nonlinear process of the wave self-diffraction in the case of the nonlocal response can be described by the sine-Gordon equation [10–13]. The variable of the sine-Gordon equation is the integral under the grating amplitude profile. It is known well that the sine-Gordon equation together with the nonlinear Schrödinger and Korteweg-de Vries ones possesses the soliton solutions [14]. We have derived that the grating amplitude has a soliton shape in the spatial direction of the wave propagation. In steady state the shape of the soliton is determined by the input intensity ratio of recording beams.

We present some experiments on the measurement of the nonuniform distribution of the grating amplitude profile across the crystal and of its dependence of input intensity ratio. For this measurement we propose a different experimental setup that uses an expanded probe beam covering completely the upper surface of the crystal sample, incident from a Bragg direction of the grating planes, but not in the plane of the recording beams. Since there is no vertical position dependence in the distribution of the spatial grating, all points of the diffracted pattern of the probe beam has a proportional intensity to the square of the magnitude of the refractive index grating at the respective horizontal position. (The effect of the deviation of the probe beam from the vertical direction inside the crystal is negligible in our case due to the large value of the refractive index). The experimental results are in good qualitative agreement with the theoretical calculations of the soliton profile.

In the developed theoretical description all solutions for output intensities are derived from the grating amplitude solution, which is determined by the intensity ratio of the input waves. By changing the input intensity ratio, the grating amplitude shape changes as well, and this way all output parameters of the FWM scheme change, too. In addition to stationary soliton solutions we have obtained multisoliton behavior

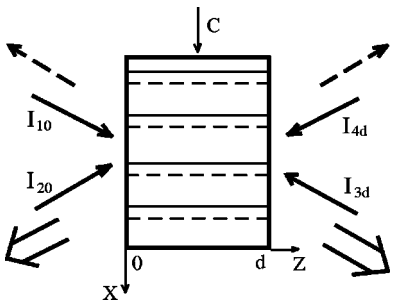

FIG. 1. The four-wave mixing scheme with symmetrical transmission geometry. The nonlocal phase grating (dashed lines) is shifted relative to the maximum intensities of the light interference pattern (solid lines). *C* is the crystal polar axis.

by numeric calculations. They show auto-oscillations of the grating and as a consequence they lead to auto-oscillations of all output wave intensities. The possibility of their existence has a basis in the fact that a local component of the grating appears and it leads to mutual changes of phases of interacted waves. As a result, the grating indexes are inclined in the crystal volume and a stationary grating cannot be recorded.

The present model of grating dynamics can be used in the description with lot of phenomena and applications of dynamic holography with photorefractive media. Furthermore, it can be applied for designing new applications, for example, in signal processing, in optical switching, in optical logic, in interferometer and sensor devices.

II. THE SINE-GORDON EQUATION IN TRANSMISSION FOUR-WAVE MIXING

In the following we consider a degenerate four-wave mixing in symmetrical transmission geometry (Fig. 1). The *z* axis shows the crystal thickness in the direction of wave propagation. The polar crystallographic axis (*C* axis) is directed along the *x* axis of light modulation. The photoinduced refractive index grating is shifted relative to the interference pattern in the direction of the *C* axis (the dashed lines in Fig. 1). According to such determination waves 1 and 4 are amplified, and waves 2 and 3 lose energy. The *n*th wave complex amplitude is $\overline{A_n}=A_n(t,z)\exp[i\varphi_n(t,z)]$, where both the real amplitude and the phase of the wave depend on the time and on the space coordinate. We designate the intensities of input waves as I_{10}, I_{20}, I_{3d}, I_{4d}; note that the fourth wave is absent on its input ($I_{4d}=0$) in the conventional FWM. Let us assume for the simplicity that the polarizations of all interacted waves are extraordinary, although the sine-Gordon equation does not depend on the wave polarization state, but is determined by only a nonlocal response and transmission geometry of the wave interaction.

The wave self-diffraction description is conventionally reduced to the following nonlinear equation set in the assumption of slow variation amplitude of plane waves [1–13]:

$$\begin{aligned}
\partial\overline{A_1}/\partial z &= -i\,\delta\varepsilon\overline{A_2},\\
\partial\overline{A_2^*}/\partial z &= i\,\delta\varepsilon\overline{A_1^*},\\
\partial\overline{A_3^*}/\partial z &= -i\,\delta\varepsilon\overline{A_4^*},\\
\partial\overline{A_4}/\partial z &= i\,\delta\varepsilon\overline{A_3},
\end{aligned} \tag{1}$$

$$\partial\,\delta\varepsilon/\partial t=\hat{F}(\overline{A_i}\overline{A_j^*})-\delta\varepsilon/T_0. \tag{2}$$

Here $\delta\varepsilon(t,z)=|\Delta\varepsilon(t,z)|\exp[i\Psi'(t,z)]$ is the complex amplitude of the dynamic grating. We neglect here the absorption in the crystal and declare that the total light intensity is a constant: $I_0=I_1+I_2+I_3+I_4=\text{const}$. All wave amplitudes are normalized by the value of I_0. We assume the fulfillment of the phase-matching conditions: $\vec{k}_1-\vec{k}_2=\vec{k}_4-\vec{k}_3=\vec{K}$, where $\vec{k}_n$ is the *n*th wave vector and $\vec{K}$ is the grating vector. Each equation of (1) shows a change of wave amplitude during its propagation through a medium. Material equation (2) describes the grating dynamics in a photorefractive medium. The first term in the right side of Eq. (2) is an operator to describe a photorefractive response being proportional to the light intensity, and the second term reveals the grating relaxation with the relaxation time constant T_0. We neglect here the effects of grating diffusion and drift.

In the case of nonlocal response the operator of Eq. (2) can be written as $\hat{F}(|E|^2)=i\gamma\Sigma E_iE_j^*$, where γ is the amplification gain. The grating is shifted by a quarter of the space period relative to the light interference pattern that is expressed by the factor *i*. The diffusion dominant mechanism is the conventional one to record nonlocal gratings in photorefractive crystals.

We assume that γ is a constant and it determines the maximum photorefractive gain of the energy transfer. For example, γ can be found from the expression

$$\gamma=-\pi r_{33}n_e^3E_{sc}[\lambda\cos(\theta)]^{-1},$$

where E_{sc} is the maximum amplitude of the space-charge field, n_e is the average refractive index for the extraordinary waves, r_{33} is the tensor component of the electro-optical constant, λ is the wavelength, and θ is the divergence angle of the light beams relative to the normal of the input crystal surfaces.

We can write dynamic equation (2) in the following form:

$$\partial\Delta\varepsilon/\partial\tau=\gamma[\overline{A_1}\overline{A_2^*}+\overline{A_4}\overline{A_3^*}]-\Delta\varepsilon, \tag{3}$$

where $\Delta\varepsilon(\tau,z)=-i\,\delta\varepsilon(\tau,z)=|\Delta\varepsilon(\tau,z)|\exp[i\Psi(\tau,z)]$ is the shifted grating, $|\Delta\varepsilon|$ is the grating amplitude, $\Psi=\pi/2-\Psi'$, $\tau=t/T_0$, γ is normalized to the total light intensity I_0.

To solve the set (1),(3) we introduce a new real variable,

$$u(\tau,z)=\int_z|\Delta\varepsilon(\tau,\zeta)|d\zeta. \tag{4}$$

The variable $u(\tau,z)$ has the physical meaning of the photoinduced changes of the optical path length along the axis z of wave-propagation direction. In the stationary state $u(z)$ is defined by the light contrast.

Considering the time argument as a parameter, we can split set (1) in two systems: for the amplitudes and for the phase differences of copropagated waves,

$$\begin{aligned} dA_1/du &= A_2\cos(\Phi_1),\\ dA_2/du &= -A_1\cos(\Phi_1),\\ d\Phi_1/du &= \sin(\Phi_1)(A_1^2-A_2^2)(A_1A_2)^{-1}, \end{aligned} \tag{5}$$

$$\begin{aligned} dA_3/du &= A_4\cos(\Phi_2),\\ dA_4/du &= -A_3\cos(\Phi_2),\\ d\Phi_2/du &= \sin(\Phi_2)(A_3^2-A_4^2)(A_3A_4)^{-1}, \end{aligned} \tag{6}$$

where $\Phi_1=\varphi_1-\varphi_2-\Psi'$, $\Phi_2=\varphi_4-\varphi_3-\Psi'$. Systems (5) and (6) has the following initial integrals:

$$\begin{aligned} d_1 &= A_1^2+A_2^2,\\ d_2 &= A_1A_2\sin(\Phi_1),\\ p_1 &= A_3^2+A_4^2,\\ p_2 &= A_3A_4\sin(\Phi_2). \end{aligned}$$

With the help of the initial integrals we obtain the exact solutions for the intensities and the phases of four coupled waves:

$$\begin{aligned} A_1^2(z) &= \sin[\beta_1 2u(z)-C_1]\frac{\sqrt{d_1^2-4d_2^2}}{2}+\frac{d_1}{2},\\ A_2^2(z) &= d_1-A_1^2(z),\\ A_3^2(z) &= \sin\{\beta_2 2[u(z)-u_d]-C_2\}\frac{\sqrt{p_1^2-4p_2^2}}{2}+\frac{p_1}{2},\\ A_4^2(z) &= p_1-A_3^2(z),\\ \cos[\Phi_1(z)] &= \cos[\beta_1 2u(z)-C_1]\frac{\sqrt{d_1^2-4d_2^2}}{2A_1(z)A_2(z)}, \end{aligned} \tag{7}$$

$$\cos[\Phi_2(z)] = \cos\{\beta_2 2[u(z)-u_d]-C_2\}\frac{\sqrt{p_1^2-4p_2^2}}{2A_3(z)A_4(z)}, \tag{8}$$

where $u_d(\tau)=u(\tau,z=d)$, d is the thickness of the crystal sample. The constants C_1 and C_2 are defined by the following input boundary conditions:

$$C_1=\arcsin[(I_{20}-I_{10})/\sqrt{d_1^2-4d_2^2}],$$

$$C_2=\arcsin[(I_{4d}-I_{3d})/\sqrt{p_1^2-4p_2^2}],$$

$$\beta_1=\mathrm{sgn}[\cos(\Phi_{10})],$$

$$\beta_2=\mathrm{sgn}[\cos(\Phi_{2d})].$$

Φ_{10}, Φ_{2d} are the input phase differences at the crystal surfaces that can be considered relative to a phase of a starting grating.

We substitute solutions (7) and (8) as well as definition (4) into dynamic equation (3) and obtain the sine-Gordon equation with the damping term $\partial u/\partial z$:

$$\frac{\partial^2 u}{\partial\tau\partial z}+\frac{\partial u}{\partial z}=R\sin(2u+\alpha), \tag{9}$$

where the values of R and α are defined by input conditions and by the value of $u_d(\tau)$. In case of matching mutual phases $\Phi_1-\Phi_2=\{0,\pi\}$ the values of R and α can be determined from the following expressions:

$$\begin{aligned} tg(\alpha) &= \{\beta_1\sqrt{I_{10}I_{20}}+(I_{3d}+I_{4d})\sin[2u_d-\beta_2\arctan(1/\vartheta)]\}\\ &\times\{\tfrac{1}{2}(I_{20}-I_{10})+(I_{3d}+I_{4d})\\ &\times\sin[2u_d+\beta_2\arctan(\vartheta)]\}^{-1}, \end{aligned}$$

where $\vartheta=(\sqrt{I_{4d}/I_{3d}}-\sqrt{I_{3d}/I_{4d}})/2$

$$\begin{aligned} R &= \gamma\{\tfrac{1}{4}(I_{10}+I_{20})^2+\tfrac{1}{4}(I_{3d}+I_{4d})^2+\cos(2u_d)[\tfrac{1}{2}(I_{20}-I_{10})\\ &\times(I_{4d}-I_{3d})+2\beta_1\beta_2\sqrt{I_{10}I_{20}I_{3d}I_{4d}}]+\sin(2u_d)\\ &\times[\beta_2\sqrt{I_{3d}I_{4d}}(I_{20}-I_{10})-\beta_1\sqrt{I_{10}I_{20}}(I_{4d}-I_{3d})]\}^{1/2}. \end{aligned}$$

The sine-Gordon equation describes the nonlinear wave-matter interaction in the process of dynamic grating recording. As a result a soliton is generated as a stable profile of the photoinduced modulation of the refractive index. The nonlinear mechanism of the soliton formation resembles that in light self-focusing of optical spatial solitons: the refractive index modulation is deeper in that spatial area where the light contrast is higher (in the case of the spatial solitons that area is determined by the local intensity of a nonuniform light beam). But the natures of the two solitons are different. Whereas in the case of the self-focusing the wave front of a propagated beam takes the soliton profile, in our case of wave self-diffraction not the electromagnetic waves but the amplitude of the refractive index grating assumes the soliton form.

In Fig. 2 it is drawn the distributions of the interacted wave intensities and of the grating amplitude through the crystal thickness in the case of double phase conjugation mirror with equaled intensity ratios on input crystal faces

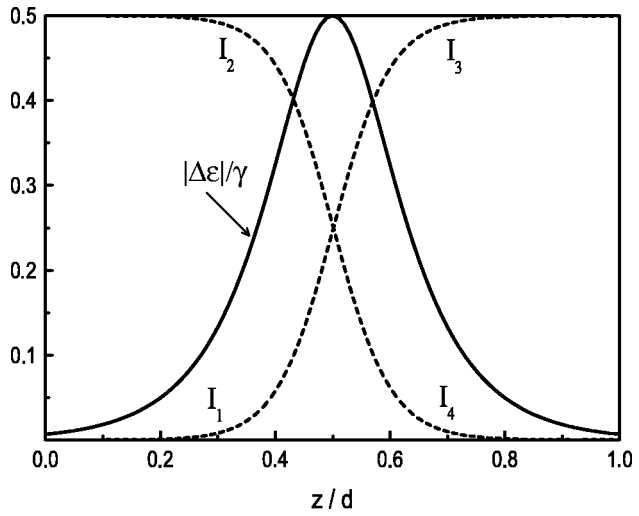

FIG. 2. Distribution of the grating amplitude and the intensities of the coupled waves along the crystal thickness. $I_{10}=I_{4d}=0$, $I_{20}=I_{3d}$; $I_0=1$, $\gamma d=10$ $|\Delta\varepsilon|/\gamma$ is the dielectric susceptibility modulation normalized to the gain constant; z/d is a distance normalized to the crystal thickness; I_n is the intensity of the nth wave normalized to the total light intensity I_0.

$(I_{10}=I_{4d}=0,\ I_{20}=I_{3d})$. In consequence of the energy transfer from the nonlocal grating the wave intensities change inside the crystal volume and the light contrast has the maximum at the point where intensities become equal. The amplitude of the photoinduced refractive index grating is proportional to the light contrast and it is described by the soliton shape. The grating amplitude maximum is located at the point of the maximal light contrast.

The temporal formation of a single soliton is shown in Fig. 3. The grating amplitude profile keeps its soliton shape at any time of grating formation, this way it can be considered as a temporal soliton. But in the special case of long time and of matching mutual phases $(\Phi_1-\Phi_2=0$ or $\pi)$, when the grating is already recorded, the grating profile becomes stable and does not change neither in time nor in space if the input conditions are held constant. The soliton becomes the spatial temporal. Just this case will be considered in the subsequent sections.

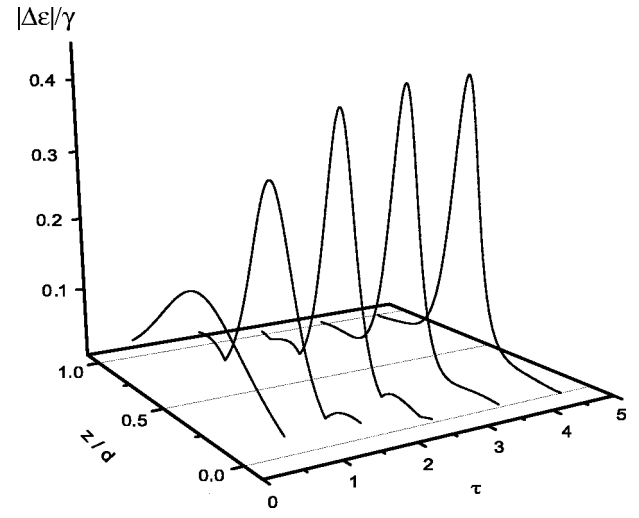

FIG. 3. The dynamics of the soliton formation. $(I_{10}/I_{20}=I_{4d}/I_{3d}=0.05;\ I_0=1;\ \gamma d=20)$. $\tau=t/T_0$ is a time normalized to the grating relaxation time T_0. The designations of $|\Delta\varepsilon|/\gamma$ and z/d are the same as in Fig. 2.

III. STATIONARY SOLITON PROFILE OF THE GRATING AMPLITUDE

In steady state equation (9) has the following solutions:

$$tg(u)=\exp(2\gamma Cz+p), \tag{10}$$

$$|\Delta\varepsilon|=\frac{\gamma C}{\cosh(2\gamma Cz+p)}, \tag{11}$$

where p and C are the constants. $\Psi=\text{const}$, i.e., the grating indexes are not inclined. The value $|\Delta\varepsilon(z)|$ determines the grating amplitude profile, the value $u(z)$ is the integral under the grating amplitude profile from 0 to z and u_d is the same integral over the crystal boundaries.

The constant C is determined by the following expression:

$$C=\tfrac{1}{2}\sqrt{H^2+4(A_1A_2+A_3A_4)^2}=\text{const},$$

where $H=|\overline{A}_2|^2+|\overline{A}_4|^2-|\overline{A}_1|^2-|\overline{A}_3|^2$.

The profile of the grating amplitude has a soliton shape. Constants p and C, which define the soliton shape, can be determined from the following input boundary conditions:

$$|\Delta\varepsilon(z=0)|=A_{10}A_{20}\cos(\Phi_{10})+A_3(0)A_4(0)\cos[\Phi_2(0)]=\frac{\gamma C}{\cosh(p)},$$

$$|\Delta\varepsilon(z=d)|=A_1(d)A_2(d)\cos[\Phi_1(d)]+A_{3d}A_{4d}\cos(\Phi_{2d})=\frac{\gamma C}{\cosh(2\gamma dC+p)}, \tag{12}$$

where $A_1(d)$, $A_2(d)$, $A_3(0)$, $A_4(0)$ are the amplitude of the output waves, $\Phi_1(d)$ and $\Phi_2(0)$ are the phase differences of output waves on the corresponding crystal faces. After substituting solutions (7) and (8) into Eq. (12), one can find the equations to determine the values C and p. The result will be the following: both constants C and p, and also the profile $|\Delta\varepsilon(z)|$ are determined by input intensity ratio, by input wave phase difference, and by the crystal photorefractive gain γ. The product γC defines the amplitude of the stationary soliton profile, the product $2C\gamma d$ determines the soliton half-width, and parameter p indicates the shift of the soliton maximum relative to the coordinate origin. The key parameter of the soliton detection is the coupling constant γd of a medium that determines the strength of the energy transfer, the light contrast changes and the soliton half-width. The soliton can be observed in those ferroelectric crystals, which

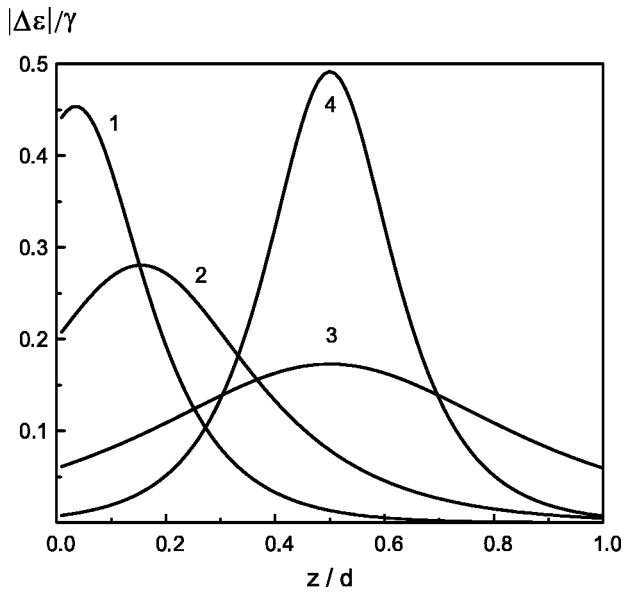

FIG. 4. Alteration of the soliton shape in steady state by changing input intensity ratios: 1—$I_{10}/I_{20}=0.1$, $I_{20}=I_{3d}=I_{4d}$; 2—$I_{10}/I_{20}=0.5$, $I_{20}=I_{3d}=I_{4d}$; 3—$I_{10}/I_{20}=I_{4d}/I_{3d}=1$; 4—$I_{10}/I_{20}=I_{4d}/I_{3d}=0.01$. ($I_0=1$; $\gamma d=10$). The designations of $|\Delta\varepsilon|/\gamma$ and z/d are the same as in the Fig. 2.

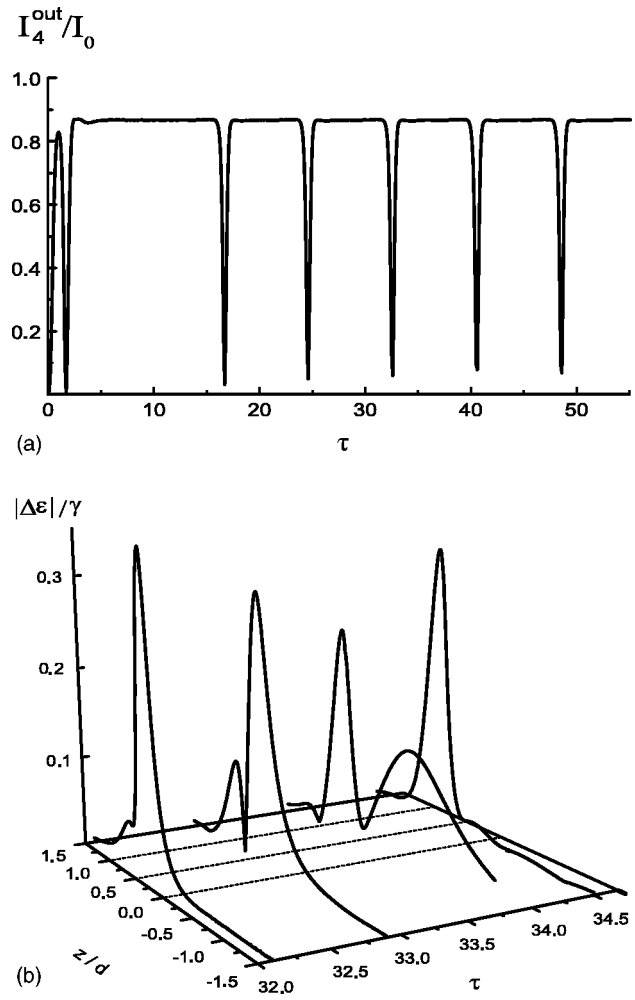

FIG. 5. (a) The oscillation of the output intensity of the phase conjugated wave in four-wave mixing scheme. $I_{10}/I_{20}=3$, $I_{3d}=0{,}87$, $I_{4d}=0$, $\gamma d=15$, ($I_0=1$). (b) The bound-soliton behavior of the dynamic grating amplitude (the input conditions is the same as in Fig. 5(a)). The designations of the normalized values are the same as in Figs. 2 and 3.

have strong photorefractive gain and a thickness more than some millimeters, e.g. $\gamma d \geqslant 10$.

The stationary soliton profiles calculated from formula (11) for the case of FWM with four input waves and for different intensity ratios are presented in Fig. 4. We determine the ratios I_{10}/I_{20} and I_{4d}/I_{3d} of copropagating waves at each input surface of the crystals, where I_{10} and I_{4d} are the intensities of those waves that have a wave-vector component directed along the polar axis c, and respectively the waves with intensities I_{20} and I_{3d} have a wave-vector component directed opposite to the polar axis. The theoretical calculations give results published in Refs. [12,15]. Only in such cases when these ratios are equaled ($I_{10}/I_{20}=I_{4d}/I_{3d}$), the soliton maximum is located exactly in the center of the crystal. When such ratio is broken ($I_{10}/I_{20}\neq I_{4d}/I_{3d}$), the soliton maximum is shifted to one of the crystal input faces. In the cases of usual FWM with three input waves the soliton maximum is located near such crystal surface where two copropagating waves enter. If FWM has four input waves, the soliton has a maximum near the surface where the corresponding ratio I_{10}/I_{20} or I_{4d}/I_{3d} is less. In addition to the location of the soliton maximum, the input intensity ratio determines the soliton half-width as well. The stationary soliton can be expanded and its localization degree can be decreased by means of increasing the ratios I_{10}/I_{20} and/or I_{4d}/I_{3d}. On the other hand, the soliton can be localized strongly in the case of $I_{10}\ll I_{20}$ or/and $I_{4d}\ll I_{3d}$ (see the curves 3 and 4 in Fig. 4).

From solutions (7) one can obtain the diffraction efficiency in the steady state as the sine-square function of the parameter u_d. For instance, the diffraction efficiency in the most common case of four-wave mixing with $I_{4d}=0$ is equal to $\eta=I_4(0)/I_{3d}=\sin^2(u_d)$. This way, the diffraction efficiency is defined by the integral under the soliton shape of the grating amplitude over the crystal boundaries. It shows a new method to the diffraction efficiency management by means of changes of the soliton shape, i.e. its amplitude, half-width, and the position shift. All these soliton parameters are determined by the ratios I_{10}/I_{20} and I_{4d}/I_{3d} on the crystal surfaces.

To complete the soliton class solutions we have to find multisoliton solutions, which describe interaction of several solitons or bond-soliton states (more general solutions) [14]. Here we would like to make the following remarks. The four-wave mixing is known as a scheme, which has instabilities and many-valued theoretical solutions [4,10,16,17]. On the other hand, the investigation of nonstable behavior of FWM by means of solving the sine-Gordon equation showed auto-oscillations for the intensities of the output waves [10]. We obtained the auto-oscillations of the output intensities by solving numerically the sine-Gordon equation with introducing any small phase fluctuation between coupled waves [Fig.

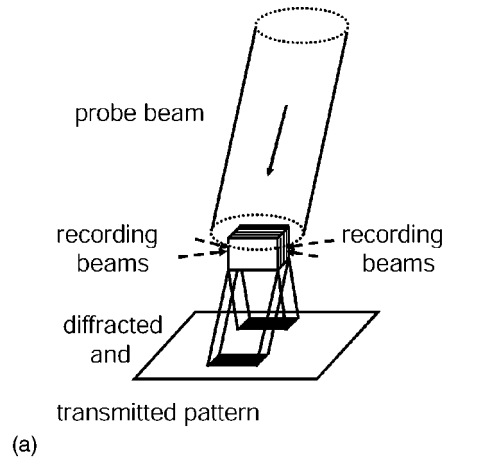

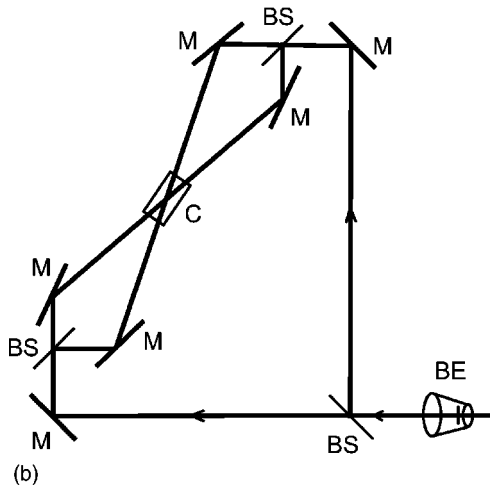

FIG. 6. (a) The experimental setup to observe the longitudinal distribution of the dynamic grating. (b) The optical scheme of four-wave mixing with four input waves. *C* is a crystal, *M* are mirrors, BS are beam splits, BE is a beam expander.

5(a)]. Those oscillations are caused by a multisoliton behavior of the grating amplitude shown in Fig. 5(b), where the evolution of two-solitons bond states during a certain time period is depicted. The auto-oscillations exist in certain regions of input intensity ratio, which are dependent on the coupling constant value [15]. They are stable to influence the phase and intensity fluctuations of recorded beams. The mechanism of the bond-soliton behavior has a basis of the emergence of a local component of the grating that leads to phase exchanges between coupled waves during their propagation. As a result, the light contrast changes with time and the grating is repeatedly erased and rerecorded. Hence the auto-oscillations can be observed only in optically reversible media.

This way the sine-Gordon mathematical approach predicts not only the stationary soliton, but also the multisoliton solutions.

IV. EXPERIMENTAL OBSERVATION OF THE NONUNIFORM DYNAMIC GRATING

To observe and measure the grating amplitude profile distribution we apply a new setup with an expanded probe beam

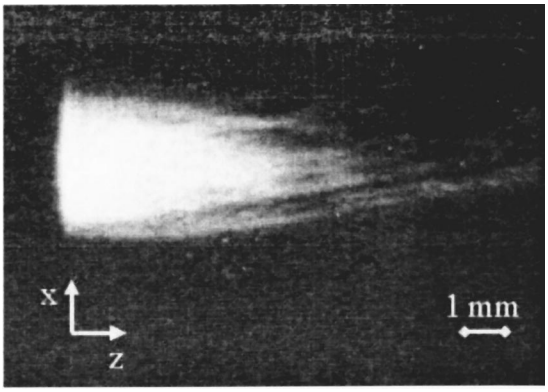

FIG. 7. The pattern of the intensity distribution of the diffracted probe beam.

incident from a Bragg direction of the grating planes, but in a plane that is perpendicular to the plane of the recording beams [Fig. 6(a)] [18]. The recorded beams are from an Ar-ion laser. We use transmission four-wave mixing scheme with symmetrical angles of incidence. The optical scheme of the recorded beams is shown in Fig. 6(b). The expanded beams are converged on the input crystal surfaces (a,c) from an angle of 12^0, where c is the optical axis of the crystals. The probe beam is from a He-Ne laser. We form a large expanded probe beam, which has uniform intensity distribution across its cross section. The probe beam enters at the Bragg angle of the grating and it covers completely the top surface (b,c) of the crystal. We can observe the patterns of both the transmitted and the diffracted output probe beams. The local value of the probe beam diffraction efficiency is proportional to the horizontal distribution of the grating amplitude point by point. This way the visual diffracted pattern is the projection of the volume distribution of the grating amplitude profile.

In present work we used $LiNbO_3$ crystals doped with 0.005 wt% Fe_2O_3 reduced to approximately OD=0.5 to let the diffusion to be the dominant mechanism of recording the grating. The crystal size was $a\times b\times c=3\times 14\times 5$ mm^3 with the thickness of 14 mm in the direction of the wave propagation. In our experiments we observed the strong light scattering in such thick crystal that takes away about 80% of the total light energy.

The typical pattern of the diffracted probe beam is shown in Fig. 7. Such pattern has been observed for the transmission four-wave mixing with three input waves and for the two-wave mixing as well. The grating amplitude is concentrated near the crystal boundary of two input waves, and there is an active energy transfer in this part. The light contrast is depleted completely beyond a thickness of about 5 mm and there is no grating and no diffracted beam in the rest part of the crystal.

Figure 8 shows the measured intensities of the diffracted probe beam along the crystal thickness in the case of four input waves for different input intensity ratios. The observed intensity fluctuations are connected with heterogeneities in the crystal volume and the light scattering. One can see that the situation is dramatically changed with four coupled waves including into the interaction. When four input waves

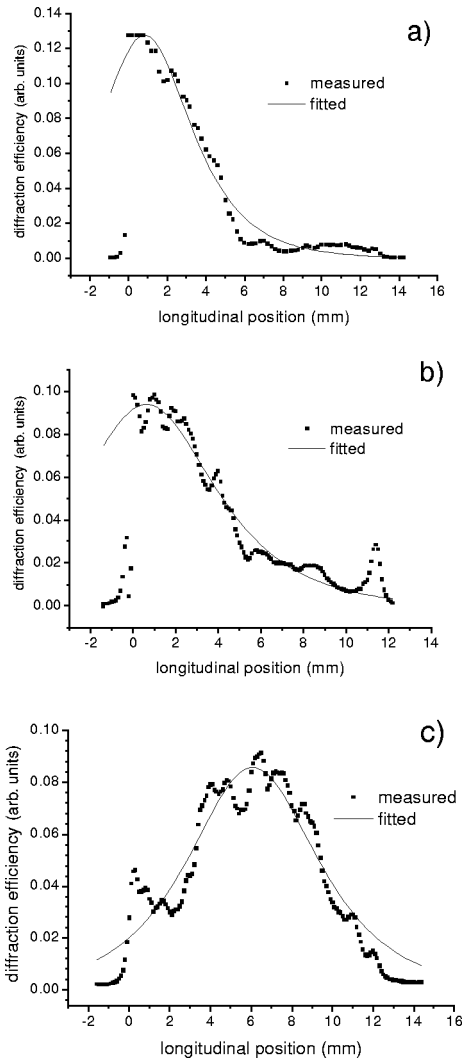

FIG. 8. The measured intensities of the diffracted probe beam along the crystal thickness. (a)—$I_{10}/I_{20}=0.08$, $I_{20}=I_{3d}=I_{4d}$; (b)—$I_{10}/I_{20}=0.14$, $I_{20}=I_{3d}=I_{4d}$; (c)—$I_{10}/I_{20}=I_{4d}/I_{3d}=1$.

have equal intensities, the active energy transfer is arisen just in the center of the crystal, and there is the maximum of the location of the grating amplitude there. This process is not obvious, but it corresponds to the theoretical prediction of the soliton formation. We obtained experimentally the maximum of the grating amplitude in the center of the crystal for that case [Fig. 8(c)].

The location of the grating amplitude maximum is changed versus the input intensity ratio. With decreasing the intensity I_{10} the grating maximum moved towards that crystal surface where input waves 1 and 2 enter, in accordance with the theory ($I_{10}/I_{20}<I_{4d}/I_{3d}$, see Sec. III). The theoretical graphs in Fig. 4 are calculated approximately for the same input intensity ratio as in the experiments (Fig. 8) in order to compare theoretical and experimental grating amplitude profiles. One can see that the experimental behavior of the grating amplitude distribution versus input intensity ratio is in good qualitative agreement with the theoretical model, describing the soliton profile.

V. CONCLUSION

The wave self-diffraction from a nonlocal phase grating in photorefractive media can be described by the sine-Gordon equation in the case of transmission geometry. The sine-Gordon equation reveals the grating amplitude dynamics induced by laser beam interaction. The grating amplitude distribution has a soliton shape in the direction of the wave propagation.

We measured experimentally the grating amplitude distribution in the volume of a photorefractive crystal. We observed the alteration of the grating amplitude profile by means of changes of the input intensity ratio. To provide such experiments we applied a different experimental setup with an expanded probe beam that entered on the investigated crystal at the Bragg angle on the surface being perpendicular to the input surfaces of recording beams. The diffracted pattern of the probe beam displays the information about the amplitude distribution of the recorded grating in the crystal volume. We showed experimentally in steady state that the changes of the grating amplitude profile versus input intensity ratio correspond to single soliton solution of the sine-Gordon equation described the FWM process. The stationary grating shape is tolerant to fluctuations of wave intensities or phases. To confirm the real soliton behavior one has to detect the time dependence of the soliton profile and its driving in accordance with the sine-Gordon equation. One possibility for the experimental verification can be the use of a pulse radiation for grating recoding (or erasing) with simultaneous detection of the grating amplitude profile in time.

The crucial parameter of the soliton is the energy transfer gain at a given distance d in the medium. The photorefractive gain determines the change of the light contrast during the wave propagation and this way the soliton localization degree as well. In the steady state the soliton is motionless and its parameters, i.e., the value and the position of the maximum, and the half-width are unequivocally defined by the input intensity ratio. The total change of the photoinduced refractive index is defined by the integral under the soliton shape of the grating amplitude and it determines the wave-mixing diffraction efficiency. Alteration of the soliton shape by means of the changes of the input intensity ratio introduces a new method to control the output wave parameters. It can be applied in all-optical signal and information processing, in optical switching and steering, and in optical logic. We obtained a multisoliton behavior that leads to auto-oscillations of output intensities. The auto-oscillations have found new applications, e.g., in interferometer devices, in optical information processing.

ACKNOWLEDGMENTS

The authors wish to thank Dr. Tatiana Davidova and Dr. Yuriy Koblyanskiy for helpful discussions about solitons in experimental physics. This research was supported by OTKA Contract No. T26088, by the Austrian-Hungarian Intergovernmental S&T Program A-8/2001, and by the Center of Excellence Program ICA1-CT-2000-70029.

[1] *Photorefractive Materials and Their Applications I*, edited by P. Gunter and J.-P. Huignard (Springer-Verlag, Berlin, 1989).
[2] S. Odoulov, M. Soskin, and A. Khizhnyak, *Optical Oscillators with Degenerate Four-Wave Mixing* (Harwood, Chur, Switzerland, 1991).
[3] *Photorefractive Materials and Their Applications II*, edited by P. Gunter and J.-P. Huignard (Springer-Verlag, Berlin, 1988).
[4] M. Cronin-Golomb, B. Fisher, J.O. White, and A. Yariv, IEEE J. Quantum Electron. **QE-20**, 12 (1984).
[5] P. Yeh, *Introduction to Photorefractive Nonlinear Optics* (Wiley, New York, 1993).
[6] *Photorefractive Optics. Materials, Properties, and Applications*, edited by Yu. Francis and Yin Shizhuo (Academic Press, New York, 2000).
[7] D.W. Vahey, J. Appl. Phys. **46**, 3510 (1975).
[8] V.L. Vinetski *et al.*, Ferroelectrics **22**, 949 (1979).
[9] D.I. Steselko and V.G. Sidorovich, Sov. Phys. JETP **44**, 580 (1974).
[10] A. Bledowski, W. Krolikowski, and A. Kujawski, J. Opt. Soc. Am. B **6**, 1544 (1989).
[11] M. Jaganathan, M.C. Bashaw, and L. Hesselink, J. Opt. Soc. Am. B **12**, 1370 (1995).
[12] S. Bugaichuk and A. Khizhnyak, J. Opt. Soc. Am. B **15**, 2107 (1998).
[13] S. Bugayhcuk and A. Khizhynak, Proc. SPIE **3904**, 201 (1999).
[14] R. K. Dodd, J. C. Eilbeck, J. D. Gibbon, and H. C. Morris, *Solitons and Nonlinear Wave Equations* (Harcourt Brace Jovanovich, New York, 1982).
[15] S. Bugaychuk and A. Khizhnyak, J. Opt. B: Quantum Semiclassical Opt. **2**, 451 (2000).
[16] W. Krolikowski, K.D. Shaw, M. Cronin-Golomb, and A. Bledowski, J. Opt. Soc. Am. B **6**, 1828 (1989).
[17] A. Zozulya and V.T. Tikhonchuk, Phys. Lett. A **135**, 447 (1989).
[18] S. Bugaychuk *et al.*, Radiat. Eff. Defects Solids (to be published).